

Numerical Study on Wave Run-up to Identify the Most Effective Design of Jakarta's Outer Sea Dike

Ikha Magdalena^{a,b,*}, Felicia Joanna Sutjianto^a, Harry Sunaryan^a, Raynaldi La'lang^a, Mohammad Farid^b, Muhammad Syahril Badri Kusuma^b, Mohammad Bagus Adityawan^b

^a Faculty of Mathematics and Natural Sciences, Bandung Institute of Technology, Jalan Ganesha No. 10, Bandung, 40132, Indonesia

^b Center for Coastal and Marine Development, Bandung Institute of Technology, Jalan Ganesha No. 10, Bandung, 40132, Indonesia

Corresponding author: *ikha.magdalena@math.itb.ac.id

Abstract— The National Capital Integrated Coastal Development (NCICD) is a construction megaproject around Jakarta Bay targeted environmental revitalization and flood mitigation. One of the main projects of NCICD is to develop the Jakarta's outer sea dike to prevent future disasters triggered by the increase of the sea level around Jakarta Bay. In this paper, we aim to assess and optimize the design of Jakarta's outer sea dike by investigating the wave run-up phenomenon, which is measured as the maximum vertical extent of wave uprush on a structure above the still water level. We used the Non-linear Shallow Water Equations (NSWE) as our mathematical model to simulate this phenomenon. The NSWE model was solved numerically using the finite volume method on a staggered grid with a wet-dry procedure to obtain accurate wave run-up height. To validate our numerical scheme, we conducted benchmark tests against a publicized experimental dataset, resulting in a good agreement between the numerical and experimental data, which confirms the robustness and accuracy of our model. We then simulate the wave run-up over three different sea dike profiles: single slope, single berm, and single berm with rocks. Our study shows that among the cases we investigated, the single berm with rocks is the most effective design of the sea dike as even small-sized rock units can significantly reduce the wave run-up height.

Keywords— Run-up; overtopping; regular wave; non-linear shallow water equations.

Manuscript received 22 Jul. 2020; revised 28 May 2021; accepted 22 Jul. 2021. Date of publication 28 Feb. 2022.
IJASEIT is licensed under a Creative Commons Attribution-Share Alike 4.0 International License.



I. INTRODUCTION

Indonesia is ranked as the third-longest coastline globally, with a total length of 54,716 km [1]. It is estimated that 60% of Indonesia's total population occupies coastal areas (within 50 km from the coastline). This number is expected to rise to about 73% by 2055 [2]. In addition, more than 80% of the country's industrial sites are also located in coastal areas. Particularly in Jakarta, around 40% of the coastal lowland area lies below the tidal surface. With 13 rivers disembogued in Jakarta Bay, floods are unavoidable in such densely populated and low-lying regions. They can be more severe due to land subsidence caused by excessive groundwater extraction. Added to the fact that the sea level has been rising, a serious attempt to prevent more disasters is necessary. Therefore, in 2014, the Provincial Government of DKI Jakarta, Banten, and West Java, together with the Ministry for Public works and Human Settlements, launched a megaproject called NCICD (National Capital Integrated Coastal Development), which includes the development of Jakarta's outer sea dike.

Several studies have been undertaken to analyze various aspects of this project. One evaluated the project in the grand scheme of things [3], another focused on watershed management studies for flood mitigation [4], and the other studied sea defense structures related to this project [5]. However, those studies did not consider one significant aspect that is very useful when investigating the sea dike structure, which is the wave run-up phenomenon. Wave run-up is the phenomenon that occurs when an ocean wave reaches a beach or sea dike structure and rises above the still water level. The height of wave run-up, which is heavily dependent on the design of the sea dike structure, may be used to assess the effectiveness of that structure. As a result, calculating wave run-up height would be highly beneficial in identifying the optimal sea dike design. This subject is discussed further in this paper.

Previously, several researchers have studied the wave run-up phenomenon experimentally [6]–[9]. However, the experimental method is proven to be costly and prone to high overheads. Therefore, there have been several attempts to

investigate wave run-up empirically for a certain bathymetry. Lerma *et al.* [10] developed a model to reproduce wave run-up in highly dissipative stormy conditions. Whilst these results are pragmatic and efficient in modeling reality, they are difficult to generalize because they are usually calibrated to a certain condition. Several studies constructed empirical formulae which are only suited for certain bottom topographies [11]–[15]. A numerical model, on the other hand, is undoubtedly applicable in a variety of situations.

A popular model in fluid dynamics to be approached numerically is the Navier-Stokes equations [16]–[20]. Despite their high accuracy, these equations are not entirely practical for modeling since they are complicated and require finer grids to simulate, making them computationally expensive [21]. Another model that could be used is the Boussinesq-type equations [22]–[27]. Solving these equations requires dealing with higher-order derivative terms, which are difficult to handle.

Therefore, we develop a numerical model of Nonlinear Shallow Water Equations (NSWE) to study wave run-up over various sea dike designs and determine the most effective one. The NSWE model is favorable and beneficial due to its simplicity yet powerful ability to simulate different test cases with fairly accurate results. Compared to the Navier-Stokes and Boussinesq-type Equations, NSWE is much easier to solve numerically, thus, saving us computational costs. There are two ways to solve NSWE numerically: using a collocated grid [28] and a staggered grid [29]–[32]. However, using a collocated grid often leads to Riemann problems, which can be avoided by using a staggered grid instead [33]. This reason leads us to use the staggered grid finite volume method in this study.

Following the establishment of the numerical scheme, we run multiple simulations based on an experiment done by Synolakis [34]. The results were compared to the experimental data to confirm our model's accuracy. Moreover, the validated scheme was used to simulate wave run-up on three different sea dike designs: one sloping domain, two sloping domains with a berm, and two sloping domains with berm and rocks. The simulations are based on experiments performed in 2018 as part of the NCICD megaproject. The simulation results were analyzed to identify the optimum design for reducing wave run-up height. Combining the NSWE model and a staggered finite volume method offers an alternative approach to designing and evaluating the optimal design of Jakarta's outer sea dike. Furthermore, the simple yet accurate model and method used allowed researchers to solve the problems easily and accurately estimate wave run-up height for each design we assessed.

The main objective of this research is to assess and identify the optimal design of Jakarta's outer sea dike to reduce wave run-up height and avoid flooding around Jakarta Bay. A mathematical model and numerical method were applied and discussed in detail in the fifth chapter of this paper to accomplish the research objectives. We briefly introduce the wave run-up phenomenon and the model and method used in this paper in the first chapter. The formulation of the mathematical model based on the NSWE is explained in the second chapter. In the third chapter, the numerical scheme built using a staggered finite volume method is presented. Then, in the fourth chapter, we validated the numerical

scheme against experimental data and evaluated the most effective sea dike design. Finally, in the fifth chapter, we overview all the research findings and recommend the most effective design for Jakarta's outer sea dike. Furthermore, we believe that the results of this study can be used to develop one of the optimization tools for the design of a sea dike structure.

II. MATERIAL AND METHOD

This study was performed in several steps, starting from examining the wave run-up phenomenon on a sea dike structure to the optimal design to minimize the wave run-up height. Several stages were pursued in the first step as formulation of the mathematical model. Then, we established a numerical scheme to solve the model. This scheme was used to simulate a specific case, the results of which were validated against previously collected experimental data. Next, the scheme was applied to simulate wave run-up on three different sea dike's designs. The results were compared to experimental data obtained specifically for the Jakarta Sea dike project, which was assessed to determine the optimal sea dike design for minimizing wave run-up height. A flowchart of this study can be seen in Fig. 1.

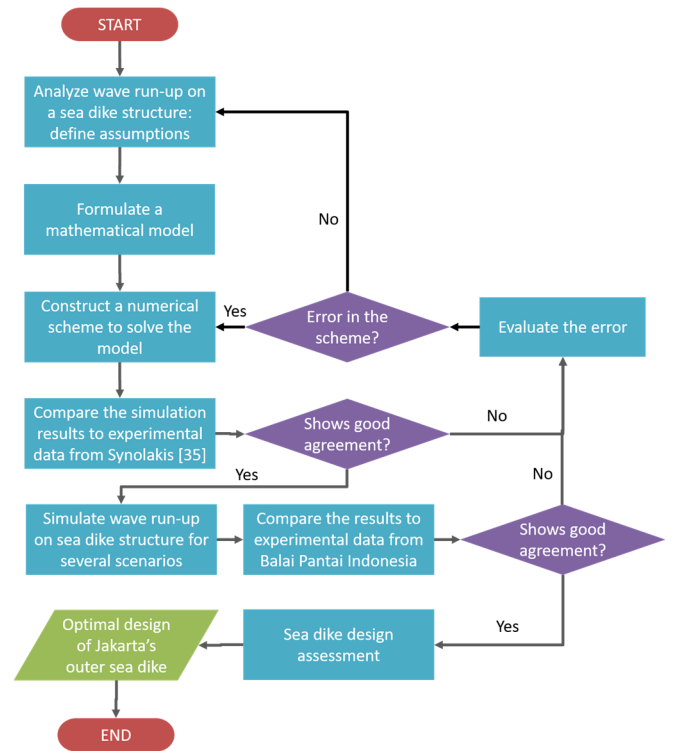


Fig. 1 Flowchart illustrating the procedure of this research.

A. Mathematical Model

In this section, we applied the Non-linear Shallow Water Equations to three different sea dike designs. The following system of differential equations governs our model:

$$\eta_t + (hu)_x = 0, \quad (1)$$

$$u_t + uu_x + g\eta_x + c_f u = 0. \quad (2)$$

Eq. (1) represents the mass conservation equation, and Eq. (2) represents the momentum balance equation in the horizontal direction. Meanwhile, uu_x is the advection term, serving as the

nonlinearity factor of this equation. The mathematical model is illustrated in Fig. 2.

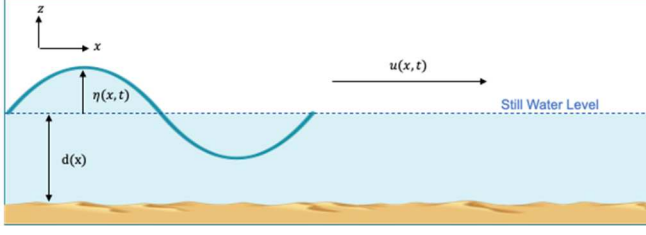


Fig. 2 Illustration for NSWE

Here, we define the governing equations of the incoming waves propagating from the sea, which result in wave run-up and overtopping over the sea dike structure. Let η denotes the surface elevation, and u is the horizontal velocity, with gravitational acceleration g . The water thickness is denoted by $h = \eta + d$, where d is the water depth measured from the still water level.

B. Numerical Method

Here, we derive the numerical solution for Eqs. (1, 2) by applying a staggered finite volume method. To start with, we define a computational domain, which comprises of a spatial domain $\Omega_L = [L_0, L_1]$ and a time domain $\Omega_T = [0, T]$. We divide the spatial domain Ω_L into half and full grids with the spatial step Δx . After that, we discretize the time domain Ω_T to finite time steps with a constant interval Δt . Next, Eqs. (1, 2) was partitioned with cells centered at x_i and $x_{i+1/2}$, respectively. As seen in Fig. 3, we calculate the water surface η and velocity u at the full- and half-grid points, respectively.

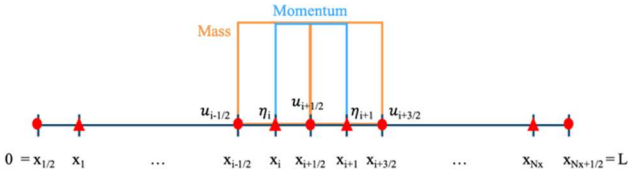


Fig. 3 Discretization of staggered conservative scheme

Then, using this partition, we obtain the difference equations for Eq. (1, 2), which are:

$$\frac{\eta_i^{n+1} - \eta_i^n}{\Delta t} + \frac{(h^*u)_{i+1/2}^n - (h^*u)_{i-1/2}^n}{\Delta x} = 0, \quad (3)$$

$$\frac{u_{i+1/2}^{n+1} - u_{i+1/2}^n}{\Delta t} + g \frac{\eta_{i+1}^{n+1} - \eta_i^{n+1}}{\Delta x} + (uu_x)_{i+1/2}^n = -c_f u_{i+1/2}^{n+1}, \quad (4)$$

where subscripts and superscripts denote the spatial grid point and time, respectively. However, referring to Eq. (3), we do not have the value of the water thickness h^* at half-grid points. Thus, we approximate h^* using the upwind method written as:

$$h_{i+1/2}^* = \begin{cases} h_i & u_{i+1/2}^n \geq 0 \\ h_{i+1} & u_{i+1/2}^n < 0 \end{cases} \quad (5)$$

Therefore, for positive flows, we have

$$\eta_i^{n+1} = \eta_i^n - \frac{\Delta t}{\Delta x} \left(h_i^n u_{i+1/2}^n - h_{i-1}^n u_{i-1/2}^n \right). \quad (6)$$

Additionally, to ensure that our numerical scheme is stable, on the right-hand side of the momentum equation (Eq. 2), η is evaluated at t_{n+1} , in place of t_n . The most difficult part in

solving NSWE is approximating the advection term. Here, the advection term uu_x is obtained from the relation $q = hu$, written as

$$uu_x = \frac{1}{h} \left(\frac{\partial(qu)}{\partial x} - u \frac{\partial q}{\partial x} \right). \quad (7)$$

Next, we discretize Eq. (7) as follow:

$$(uu_x)_{i+1/2} = \frac{1}{\bar{h}_{i+1/2}} \left(\frac{\bar{q}_{i+1}^* u_{i+1} - \bar{q}_i^* u_i}{\Delta x} - u_{i+1/2} \frac{\bar{q}_{i+1} - \bar{q}_i}{\Delta x} \right), \quad (8)$$

with

$$\bar{h}_{i+1/2} = \frac{1}{2} (h_i + h_{i+1}), \quad (9)$$

$$\bar{q}_i = \frac{1}{2} (q_{i+1/2} + q_{i-1/2}), \quad (10)$$

$$^*u_i = \begin{cases} u_{i-1/2} & \bar{q}_i \geq 0 \\ u_{i+1/2} & \bar{q}_i < 0 \end{cases} \quad (11)$$

To simulate wave propagation over a sloping structure h where we have a moving boundary over a dry area, it is necessary for the numerical scheme to adapt to the moving wet-dry interface. Therefore, we compute the discrete formula for Eq. (4) only if the water depth is greater than a minimum threshold depth $h_{min} = 0$.

III. RESULT AND DISCUSSION

Here, we present several numerical simulations and analyze their ability to estimate wave run-up height. For validation, the numerical results was compared to the experimental data provided by Synolakis [34]. Following that, we run simulations for three different sea dike structures: one sloping domain, two sloping domains with a berm, and two sloping domains with berm and rocks. The results were compared to the experimental data from the NCICD. Further, simulations with various friction coefficients were conducted to identify the optimal size of rocks on the sea dike.

A. Comparison with Synolakis' Experiment

First, we examined the ability of our numerical scheme to model wave propagation with the existence of nonlinearity and wet-dry conditions. Here, we use the data from Synolakis' experiment of a solitary wave propagating through a single slope as our benchmark test. Our numerical scheme uses the same initial wave as the Synolakis' experiment, which was done in a wave tank with 31.73 m of length, 39.97 cm of width, and 60.96 cm of depth. Considering that the length of the wave tank is much longer than the width, we can validate our one-dimensional numerical scheme with this experimental data. Here, we use the initial condition as follow:

$$\eta(x, 0) = A \operatorname{sech}^2(\gamma(x - x_0)),$$

$$u(x, 0) = \sqrt{\frac{g}{d_0}} \eta(x, 0),$$

where A is the wave height, d_0 is the undisturbed water depth, x_0 is the wave crest position, and $\gamma = \sqrt{\frac{3A}{4d_0}}$. We set two simulations with $d_0 = 1$, the first of which is the non-

breaking solitary wave with $A = 0.0185$, and $x_0 = 38.34$. The second one is the solitary breaking wave. For the numerical simulations, we choose $\Delta x = 0.3$ and $\Delta t = 0.003$.

Figure 4 compares the experiment measurement (dashed line) and numerical results (solid line) for $t = 40, 50, 60, 70$ s. The key takeaway from this figure is that our numerical scheme can accurately simulate the phenomenon seen in Synolakis' experiment. Therefore, we proceed the comparison with a larger normalized wave height, $A/d_0 = 0.3$. We compare the results at $t = 15, 20, 25, 30$ s, as shown in Fig. 5.

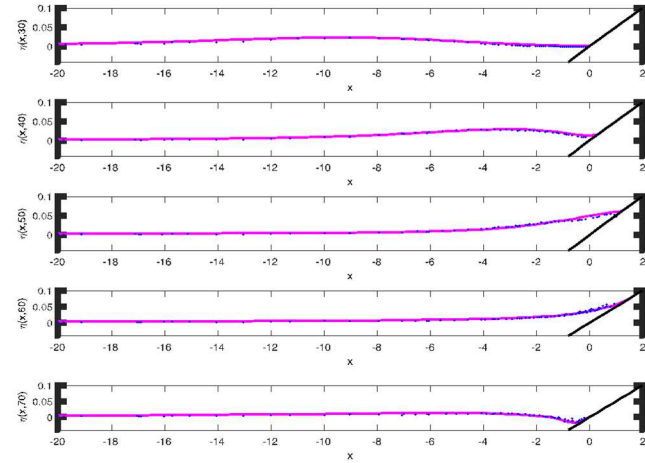


Fig. 4 Wave surface profile for $A/d_0 = 0.0185$ at (a) $t = 40$, (b) $t = 50$, (c) $t = 60$, (d) $t = 70$

From Fig. 4 and Fig. 6, we can slightly notice that in the first half of both experiments, our computational scheme underestimated the wave profile before and after it reached the beach. However, near the shoreline tip, our numerical scheme slightly overestimated the wave run-up height. This is expected as in real occurrences, the viscous effects are most significant in that flow region, while we ignore this effect in the model [34]. Nevertheless, we can infer from both figures that our numerical scheme successfully simulated the wave run-up phenomenon.

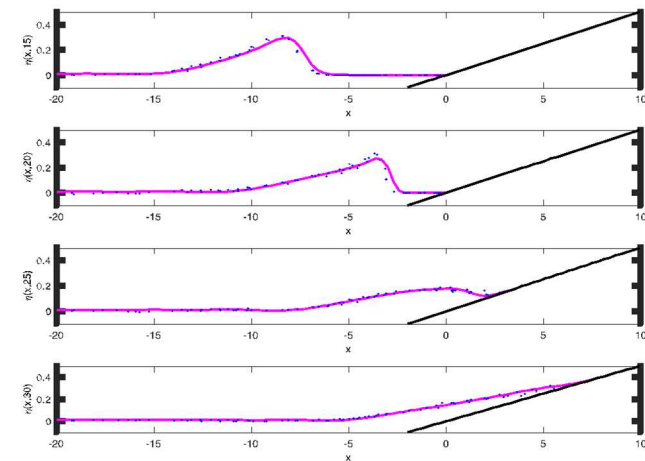


Fig. 5 Wave surface profile for $A/d_0 = 0.3$ at (a) $t = 15$, (b) $t = 20$, (c) $t = 25$

B. Simulation Cases with Experimental Data

Now that we have confirmed our numerical scheme's ability to perform the wave run-up phenomenon simulation, we investigated further the Jakarta outer sea dike design. In

this case, we compared our numerical results with the experimental data from Balai Pantai Experiment. This experiment was conducted in a scale of 1:30 with the scaling of length and time was determined by Froudian similitude.

We tested our numerical scheme for multiple scenarios by varying the wave amplitude and period. The numerical scheme's performance is evaluated using MAPE (Mean Absolute Percentage Error) and RMSE (Root Mean Squared Error) metrics defined as the following:

$$MAPE = \frac{1}{n} \sum_{i=1}^n \left| \frac{A_i - P_i}{A_i} \right|,$$

$$RMSE = \sqrt{\frac{1}{n} \sum_{i=1}^n (A_i - P_i)^2}.$$

The variable n denotes the number of scenarios, A_i and P_i denote the experimental and numerical results of run-up phenomena, respectively.

1) *Single Slope (SD1)*: First, we tested the simulation to examine the numerical scheme's performance to model wave propagation over a single slope. We use the same initial wave as the experiment on wave transformation and wave-structure interaction processes, which was conducted in a wave flume at Laboratory of Experimental Station for Coastal Engineering Buleleng, Bali. Considering that the length of the wave tank is much longer than the width, we can validate our scheme with this experimental data. In this case, we perform the numerical simulation based on the illustration in Fig. 6. The length of each domain is $\Omega_1 = 15$ m, $\Omega_2 = 2.775$ m, and $\Omega_3 = 0.655$ m.

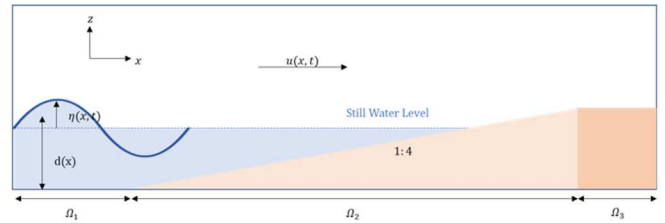


Fig. 6 Experiment Set-up Case for Single Slope (SD1)

TABLE I
RESULT CASE FOR SINGLE SLOPE

Amplitude (m)	Period (s)	Experimental Run-up (m)	Numerical Run-up (m)
0.025	1.0	0.1097	0.1000
0.050	1.0	0.1920	0.2125
0.050	1.5	0.2236	0.2750
0.065	1.5	0.2868	0.3375
0.080	1.5	0.3343	0.3375
0.050	2.0	0.2394	0.3000
0.050	2.0	0.2394	0.3000
0.050	2.0	0.2394	0.3000

Table I has the RMSE and MAPE values for the experimental and numerical results, which are 0.052 and 0.17, respectively. Those numbers show that the ability of our numerical scheme to simulate run-up phenomena is passable. However, we need to examine other cases below to provide a more accurate conclusion about our numerical scheme.

2) *Single Berm (SD2)*: In this case, we increase the number of domains by introducing a berm and a second sloping domain. We create the numerical scheme based on the illustration in Fig. 7, where each domain has length of $\Omega_1 = 15\text{ m}$, $\Omega_2 = 2.8\text{ m}$, $\Omega_3 = 0.33\text{ m}$, $\Omega_4 = 0.84\text{ m}$, and $\Omega_5 = 0.5\text{ m}$.

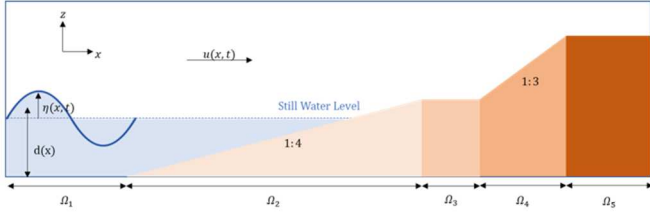


Fig. 7 Experiment Set-up Case for Single Berm (SD2)

According to the results presented in Table II, the RMSE and MAPE values for the experimental and numerical results are 0.085 and 0.159, respectively. The number of MAPE is lower than the previous simulation, but the number of RMSE is higher. Those numbers show that the effects of extreme values cannot be ignored, but the overall performance is better.

TABLE II
RESULT CASE FOR SINGLE BERM

Amplitude (m)	Period (s)	Experimental Run-up (m)	Numerical Run-up (m)
0.025	1.0	0.1095	0.1000
0.050	1.0	0.1825	0.1750
0.050	1.5	0.1825	0.1840
0.065	1.5	0.2775	0.2940
0.080	1.5	0.2775	0.3607
0.050	2.0	0.4200	0.2607
0.065	2.0	0.2775	0.3273
0.080	2.0	0.3725	0.4273
0.050	2.5	0.3725	0.2940
0.065	2.5	0.3725	0.3607
0.080	2.5	0.6650	0.4607

3) *Single Berm with Rocks (SD3)*: In the previous cases, we did not consider friction on the surface of the sea dike. However, interactions between sea dike and waves in real life generate friction, which cannot be ignored. The measure of friction in a sea dike depends on the materials used to build the structure. For this case, we introduce friction by adding rocks. We assumed that the rocks are well-distributed over the sea dike structure and have a median diameter of 66 cm, which converts into friction coefficient of 0.266 by this formula: $c_f = 0.041 \sqrt[6]{d_{50}}$, where c_f denotes the friction coefficient and d_{50} denotes the median diameter of rocks. The illustration for this case can be found in Fig. 8.

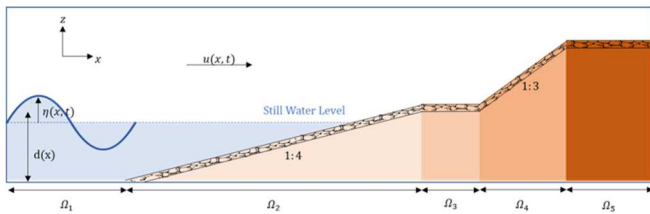


Fig. 8 Experiment Set-up Case for Single Berm with Rocks (SD3)

From Table III, the RMSE and MAPE for the experimental and numerical results are 0.0087 and 0.039, respectively. Those numbers show that our numerical scheme predicts the run-up phenomenon accurately. Furthermore, the fact that the

number of RMSE is closer to zero than the other sea dike design indicates no significant differences between the experimental and numerical wave run-up.

TABLE III
RESULT CASE FOR SINGLE BERM WITH ROCKS

Amplitude (m)	Period (s)	Experimental Run-up (m)	Numerical Run-up (m)
0.025	1.0	0.1095	0.0840
0.050	1.0	0.1095	0.1077
0.050	1.5	0.1095	0.1077
0.065	1.5	0.1095	0.1094
0.080	1.5	0.2045	0.2006
0.050	2.0	0.1095	0.1147
0.065	2.0	0.2045	0.2060
0.080	2.0	0.2045	0.2060
0.050	2.5	0.1825	0.1802
0.065	2.5	0.1825	0.1747
0.080	2.5	0.2995	0.2917

C. Sea Dike Design Assessment

1) *Sea Dike Profile*: To assess each design, we compare the relation between wave amplitude and run-up in SD1, SD2, and SD3, as illustrated in Fig. 9. Overall, SD3 is the sea dike profile that reduces the wave run-up height most effectively. This finding infers those rocks are indeed effective in reducing wave run-up. Therefore, we further investigated the most effective size of rocks to be used in sea dike design.

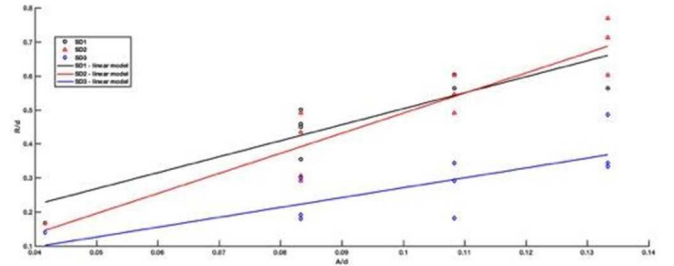


Fig. 9 Comparison of Sea Dike Profiles

2) *Different Sizes of Rocks*: For the last simulation, we try to simulate the numerical scheme for the same sea dike structure with a single berm, but with various sizes of rocks.

TABLE IV
RESULT CASE FOR SINGLE BERM WITH ROCKS

d_{50} (m)	c_f	Run-up (m)
0.0000	0.0000	0.2145
0.0000	0.0021	0.1794
0.0002	0.0096	0.1445
0.0010	0.0130	0.1094
0.0040	0.0164	0.1094
0.0168	0.0207	0.1094
0.0840	0.0271	0.1094

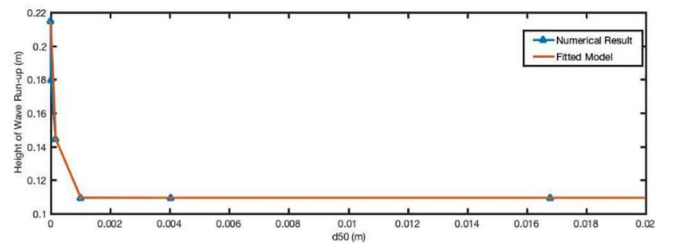


Fig. 10 Influence of d_{50} towards the Height of Wave Run-up

As seen in Fig. 10, the relationship appears to look like an exponential decay which can be fitted into this formula:

$$R = 0.1051 e^{-6543.3x} + 0.1094$$

Increasing the size of rocks indeed reduced run-up. However, after a certain point (in this case, $d_{50} = 0.001\text{ m}$), this declining trend starts to become insignificant and instead turns stagnant. This would mean that larger rocks are better at reducing run-ups. However, it gets to the point where increasing the size of rocks does not affect much. One should then choose the appropriate rock sizes by considering the cost of installation and maintenance.

IV. CONCLUSION

We have successfully simulated the wave run-up phenomenon using a numerical scheme derived from the Nonlinear Shallow Water Equations. Several test cases against the experimental data have been performed to examine the accuracy of our scheme. Among the three sea Dike designs that are evaluated, our scheme can simulate run-up phenomena more precisely on structures with rocks (SD3). In addition, we also found that SD3 is the most effective sea Dike design to reduce the wave run-up height. These results suggest that the friction coefficient should not be neglected, which has prompted us to investigate further the effect of rocks size on reducing wave run-up height.

The numerical scheme is used to determine the relationship between the median diameter of rocks and the wave run-up height. It is found that larger rocks are more effective in reducing wave run-up. However, one should be aware that the wave run-up height eventually remains stagnant as the rocks become larger. Hence, we should begin assessing the size of the rocks from a cost-efficiency perspective. We believe that the results of this study can be implemented as one of the assessment tools to build the optimal sea Dike structure.

ACKNOWLEDGMENT

We thank Larasari *et al.* that provide preliminary research related to this current study. The authors also want to acknowledge the funding from Bandung Institute of Technology.

REFERENCES

- [1] Central Intelligence Agency, "The World Factbook," 2021.
- [2] World Bank, "Strengthening the Disaster Resilience of Indonesian Cities – A Policy Note," World Bank, Washington, D. C., 2019.
- [3] A. Widodo, "Analyzing Indonesia's NCICD Project to Stop the Capital City Sinking," *Otoritas J. Ilmu Pemerintah.*, vol. 7, no. 2, pp. 54–66, 2017, doi: 10.26618/ojip.v7i2.769.
- [4] C. Asdak, S. Supian, and Subiyanto, "Watershed management strategies for flood mitigation: A case study of Jakarta's flooding," *Weather Clim. Extrem.*, vol. 21, pp. 117–122, Sep. 2018, doi: 10.1016/j.wace.2018.08.002.
- [5] H. Suprayogi, A. Rudyanto, H. Bachtiar, and L. M. Limantara, "Critical-phase sea dike construction of NCICD program in Jakarta as national capital city," *IOP Conf. Ser. Earth Environ. Sci.*, vol. 162, no. 1, p. 12020, 2018, doi: 10.1088/1755-1315/162/1/012020.
- [6] D. Di Luccio, G. Benassai, G. Budillon, L. Mucirino, R. Montella, and E. Pugliese Carratelli, "Wave run-up prediction and observation in a micro-tidal beach," *Nat. Hazards Earth Syst. Sci.*, vol. 18, no. 11, pp. 2841–2857, 2018, doi: 10.5194/nhess-18-2841-2018.
- [7] F. M. Evers and R. M. Boes, "Impulse wave run-up on steep to vertical slopes," *J. Mar. Sci. Eng.*, vol. 7, no. 1, pp. 1–15, 2019, doi: 10.3390/jmse7010008.

- [8] M. A. Shermeneva, "Calculation of the sea wave run-up on a sloping beach," *Phys. Wave Phenom.*, vol. 25, no. 1, pp. 74–77, 2017, doi: 10.3103/S1541308X17010125.
- [9] H. J. Hafsteinnsson, F. M. Evers, and W. H. Hager, "Solitary wave run-up: wave breaking and bore propagation," *J. Hydraul. Res.*, vol. 55, no. 6, pp. 787–798, 2017, doi: 10.1080/00221686.2017.1356756.
- [10] A. Nicolae Lerma, R. Pedreros, A. Robinet, and N. Sénéchal, "Simulating wave setup and runup during storm conditions on a complex barred beach," *Coast. Eng.*, vol. 123, no. January, pp. 29–41, 2017, doi: 10.1016/j.coastaleng.2017.01.011.
- [11] G. V. Da Silva, P. G. Da Silva, R. S. Araujo, A. H. Da Fontoura Klein, and E. Toldo, "Wave run-up on embayed beaches. Study case: Itapocorói Bay, Southern Brazil," *Brazilian J. Oceanogr.*, vol. 65, no. 2, pp. 187–200, 2017, doi: 10.1590/s1679-87592017133706502.
- [12] A. Khoury, A. Jarno, and F. Marin, "Experimental study of run-up for sandy beaches under waves and tide," *Coast. Eng.*, vol. 144, no. September 2017, pp. 33–46, 2019, doi: 10.1016/j.coastaleng.2018.12.003.
- [13] C. Ji, Q. Zhang, and Y. Wu, "An empirical formula for maximum wave setup based on a coupled wave-current model," *Ocean Eng.*, vol. 147, no. September 2017, pp. 215–226, 2018, doi: 10.1016/j.oceaneng.2017.10.021.
- [14] A. Torres-Freyermuth, J. C. Pintado-Patiño, A. Pedrozo-Acuña, J. A. Puleo, and T. E. Baldock, "Runup uncertainty on planar beaches," *Ocean Dyn.*, vol. 69, no. 11–12, pp. 1359–1371, 2019, doi: 10.1007/s10236-019-01305-y.
- [15] G. Dodet, F. Leckler, D. Sous, F. Ardhuin, J. F. Filipot, and S. Suanez, "Wave Runup Over Steep Rocky Cliffs," *J. Geophys. Res. Ocean.*, vol. 123, no. 10, pp. 7185–7205, 2018, doi: 10.1029/2018JC013967.
- [16] Y. Yao, M. jun Jia, D. wei Mao, Z. zhi Deng, and X. jian Liu, "A Numerical Investigation of the Reduction of Solitary Wave Run-up by A Row of Vertical Slotted Piles," *China Ocean Eng.*, vol. 34, no. 1, pp. 10–20, 2020, doi: 10.1007/s13344-020-0002-z.
- [17] M. Alagan Chella, H. Bihs, D. Myrhaug, and M. Muskulus, "Breaking solitary waves and breaking wave forces on a vertically mounted slender cylinder over an impermeable sloping seabed," *J. Ocean Eng. Mar. Energy*, vol. 3, no. 1, pp. 1–19, 2017, doi: 10.1007/s40722-016-0055-5.
- [18] X. Fan, J. Zhang, and H. Liu, "Numerical analysis on the secondary load cycle on a vertical cylinder in steep regular waves," *Ocean Eng.*, vol. 168, no. April, pp. 133–139, 2018, doi: 10.1016/j.oceaneng.2018.08.064.
- [19] X. Fan, J. xin Zhang, and H. Liu, "Numerical Investigation of Run-ups on Cylinder in Steep Regular Wave," *China Ocean Eng.*, vol. 33, no. 5, pp. 601–607, 2019, doi: 10.1007/s13344-019-0058-9.
- [20] X. Zou, L. Zhu, and J. Zhao, "Numerical simulations of non-breaking, breaking and broken wave interaction with emerged vegetation using navier-stokes equations," *Water (Switzerland)*, vol. 11, no. 12, p. 2561, 2019, doi: 10.3390/w11122561.
- [21] V. Sriiram, Q. W. Ma, and T. Schlurmann, "Numerical simulation of breaking waves using hybrid coupling of fnpt and ns solvers," *Proc. Int. Offshore Polar Eng. Conf.*, vol. 4, pp. 1118–1124, 2012.
- [22] D. Adytia, S. R. Pudjaprasetya, and D. Tarwidi, "Modeling of wave run-up by using staggered grid scheme implementation in 1D Boussinesq model," *Comput. Geosci.*, vol. 23, no. 4, pp. 793–811, 2019, doi: 10.1007/s10596-019-9821-5.
- [23] J. Hao and A. Gao, "Blow-up for Generalized Boussinesq Equation with Double Damping Terms," *Mediterr. J. Math.*, vol. 17, no. 6, pp. 2–11, 2020, doi: 10.1007/s00009-020-01604-5.
- [24] C. Lawrence, D. Adytia, and E. van Groesen, "Variational Boussinesq model for strongly non-linear dispersive waves," *Wave Motion*, vol. 76, pp. 78–102, 2018, doi: 10.1016/j.wavemoti.2017.10.009.
- [25] Y. Ning, W. Liu, X. Zhao, Y. Zhang, and Z. Sun, "Study of irregular wave run-up over fringing reefs based on a shock-capturing Boussinesq model," *Appl. Ocean Res.*, vol. 84, no. January, pp. 216–224, 2019, doi: 10.1016/j.apor.2019.01.013.
- [26] W. Liu, Y. Ning, F. Shi, and Z. Sun, "A 2DH fully dispersive and weakly non-linear Boussinesq-type model based on a finite-volume and finite-difference TVD-type scheme," *Ocean Model.*, vol. 147, no. December 2019, p. 101559, 2020, doi: 10.1016/j.oceomod.2019.101559.
- [27] Y. Yao, Z. Tang, C. Jiang, W. He, and Z. Liu, "Boussinesq modeling of solitary wave run-up reduction by emergent vegetation on a sloping beach," *J. Hydro-Environment Res.*, vol. 19, pp. 78–87, 2018, doi: 10.1016/j.jher.2018.03.001.
- [28] H. Suzuki, Y. Hasegawa, M. Watanabe, U. Tatsuo, and S. Mochizuki, "Second-order kinetic energy-conservative analysis of incompressible

- turbulence under a collocated grid system,” *J. Phys. Conf. Ser.*, vol. 1633, no. 1, p. 012063, 2020, doi: 10.1088/1742-6596/1633/1/012063.
- [29] I. Magdalena, “Non-hydrostatic model for solitary waves passing through a porous structure,” *J. Disaster Res.*, vol. 11, no. 5, pp. 957–963, 2016, doi: 10.20965/jdr.2016.p0957.
- [30] I. Magdalena, Iryanto, and D. E. Reeve, “Free-surface long wave propagation over linear and parabolic transition shelves,” *Water Sci. Eng.*, vol. 11, no. 4, pp. 318–327, 2018, doi: 10.1016/j.wse.2019.01.001.
- [31] I. Magdalena, S. R. Pudjaprasetya, and L. H. Wiryanto, “Wave interaction with an emerged porous media,” *Adv. Appl. Math. Mech.*, vol. 6, no. 5, pp. 680–692, 2014, doi: 10.4208/aamm.2014.5.s5.
- [32] I. Magdalena and H. Q. Rifatin, “Analytical and numerical studies for harbor oscillation in a semi-closed basin of various geometric shapes with porous media,” *Math. Comput. Simul.*, vol. 170, pp. 351–365, 2020, doi: 10.1016/j.matcom.2019.10.020.
- [33] T. Goudon, J. Llobell, and S. Minjeaud, “A Staggered Scheme for the Euler Equations,” in *Finite Volumes for Complex Applications VIII - Hyperbolic, Elliptic and Parabolic Problems. FVCA 2017. Springer Proceedings in Mathematics & Statistics*, 2017, pp. 91–99, doi: 10.1007/978-3-319-57394-6_10.
- [34] C. E. Synolakis, “The run-up of solitary waves,” *J. Fluid Mech.*, vol. 185, no. December 1987, pp. 523–545, 1987, doi: 10.1017/S002211208700329X.